Rare Metal Materials and Engineering
Volume 53, Issue 6, June 2024
Available online at www.rmme.ac.cn

Science Press

Cite this article as: Xu Minglei, Lu Wenli, Zhang Xiaowei, et al. Migration Laws of Impurities in Purification Process of Yttrium Metal by Plasma Zone Melting[J]. Rare Metal Materials and Engineering, 2024, 53(06): 1543-1548. DOI: 10.12442/j.issn.1002-185X.20230556.

ARTICLE

Migration Laws of Impurities in Purification Process of Yttrium Metal by Plasma Zone Melting

Xu Minglei[1,2], Lu Wenli[2,3,4], Zhang Xiaowei[1,2,3], Chen Dehong[1,2], Li Jinying[2], Yu Chuang[1,2], Yang Wensheng[2,3], Wang Zhiqiang[1,2]

[1] GRIREM Hi-Tech Co., Ltd, Langfang 065201, China; [2] GRIREM Advanced Materials Co., Ltd, Beijing 100088, China; [3] National Engineering Research Center for Rare Earth, Beijing 100088, China; [4] School of Metallurgy and Ecological Engineering, University of Science and Technology Beijing, Beijing 100083, China

Abstract: Metal Y was purified by plasma zone melting, and the migration laws of Al, Si, Fe, Ni, Cu, and Mo impurities during the zone melting purification process were obtained. Calculation results show that the equilibrium distribution coefficients of the Al, Si, Fe, Ni, Cu, and Mo impurities in metal Y are 0.2173, 0.2201, 0.5065, 0.1586, 0.1742, and 0.8576, respectively. Because all equilibrium distribution coefficients are less than 1, the solubility of impurities in the liquid phase is greater than that in the solid phase. Therefore, theoretically, with the movement of molten zone, the Al, Si, Fe, Ni, Cu, and Mo impurities will be concentrated in the tail side of Y metal ingot, namely last-to-freeze zone. Experiment results demonstrate the correctness of the theoretical calculation. Besides, the internal relationship between the zone melting times and the impurity migration was investigated. Results show that with the increase in the zone melting time from 5 to 10, the concentration degree of impurities at the tail side of Y metal ingot is increased, i.e., the removal ratio is increased. After 10 times of zone melting, the removal ratios of Al, Si, Fe, Ni, Cu, and Mo impurities are 45.71%, 61.54%, 33.98%, 64.15%, 52.14%, and 46.28%, respectively. Because the saturated vapor pressure of the abovementioned impurities is similar to that of metal Y, impurities are difficult to be removed by the common methods. The investigation of plasma zone melting proposes a new research direction for the preparation of high purity Y.

Key words: migration laws; plasma zone melting; distribution coefficient; yttrium; removal efficiency

High purity rare earth metals are the core basic materials of rare earth functional materials and their high-end application devices, such as rare earth magnetic materials, light-emitting materials for flexible display OLED, crystal materials, functional films, and other new functional materials[1–6]. The high performance of these materials depends on the preparation and application of high purity rare earth metals. Among them, the high purity metal yttrium (Y) is widely used in the electronic devices, hydrogen storage materials, and high-performance material additives[2,7–13]. It is reported that the higher the purity of metal Y, the better the performance of the materials.

Currently, metal Y is mainly produced by the metal thermal reduction, and the absolute purity of metal Y is 98wt% – 99.8wt%[14–16]. The impurities mainly include the high-vapor-pressure materials (Ca, Mg), medium-vapor-pressure materials (Al, Fe, Si, Ni, Cu), low-vapor-pressure materials (Mo, W), and non-metallic interstitial impurities (C, O, S, N). Due to the complexity of impurity types and high chemical activity of metal Y, impurities are difficult to be removed from metal Y.

Generally, the main preparation methods of high purity Y are vacuum refining, vacuum distillation, solid-state electromigration, and electrochemical refining[2,17–20]. Among them, vacuum refining mainly removes the high-vapor-pressure impurities. Vacuum distillation can remove the impurities whose vapor pressure is greatly different from that of the main metal. Solid electromigration requires long term process, but it is more effective for the removal of C, O, and other interstitial impurities. Electrochemical refining is only effective for O impurity removal. However, all these methods have limited

Received date: September 05, 2023
Foundation item: National Key Research and Development Program of China (2022YFB3504401); National Science and Technology Major Project of China (J2019-VI-0023-0140)
Corresponding author: Lu Wenli, Ph. D., GRIREM Advanced Materials Co., Ltd, Beijing 100088, P. R. China, Tel: 0086-10-61590666, E-mail: luwenli@grirem.com

effects on the medium-vapor-pressure impurities in metal Y, such as Al, Fe, Si, Ni, and Cu. The equilibrium distribution coefficients k_0 of the abovementioned impurities are rarely reported, and they are less than 1 by thermodynamic calculation. On the basis of the preceding researches, the medium-vapor-pressure impurities (Fe, Cu, Al, Si) in metal La can be effectively removed by the plasma zone melting (PZM) method. The Al, Si, Fe, Sn, As, and Sb impurities in metal Cu can also be removed by PZM. Besides, the C, S, O, and N non-metallic impurities in metal Cr can be removed by PZM. Therefore, PZM is a potential method to remove medium-vapor-pressure impurities (Al, Fe, Si, Ni, Cu) in metal Y. This purification method ameliorates the traditional purification methods and provides new ideas for the subsequent large-scale preparation of high purity rare earth metals.

1 Experiment

The raw material metal Y was prepared by calciothermy method and purified by vacuum refining method. The contents of metal impurities were obtained by inductively coupled plasma optical emission spectrometer (ICP-OES, PerkinElmer optima 8300). The analysis result shows that the impurities mainly include Al, Si, Fe, Ni, Cu, and Mo elements. Because the Al, Si, Fe, Ni, Cu, and Mo elements have low evaporation coefficients, these impurities are the main investigation objects in this research. The contents of Al, Si, Fe, Ni, Cu, and Mo impurities are 0.014wt%, 0.0117wt%, 0.0103wt%, 0.0053wt%, 0.014wt%, and 0.0121wt%, respectively. The impurity contents of raw material metal Y are shown in Table 1.

According to Table 1, various impurities exist in the Y metal ingot. To investigate the saturated vapor pressure of these impurities and metal Y, the Antoine equation was used in this research[21]. As shown in Fig.1, the vapor pressures of Al, Si, Fe, Ni, and Cu are close to that of Y and the vapor pressure of Mo is much less than that of Y. The results indicate that these impurities can hardly be removed by the common methods.

Table 1 Impurity contents of raw material metal Y

Element	Content/$\times10^{-4}$wt%
Mg	<10
Al	140
Si	117
Ca	<10
Ti	<10
V	<10
Cr	<10
Mn	<10
Fe	103
Co	<10
Ni	53
Cu	140
W	<50
Mo	121

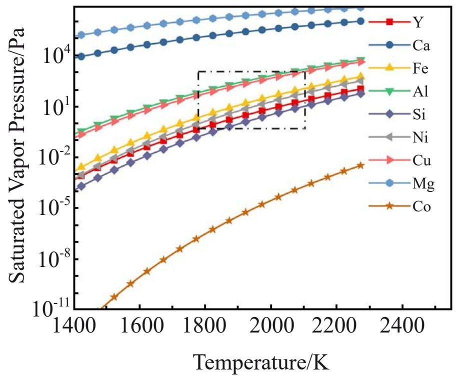

Fig.1 Saturated vapor pressures of metal Y and impurities

In this research, the self-developed and designed plasma arc melting equipment was used as PZM device, which included an arc gun, a copper crucible, a vacuum system, and a gas path system. The regional melting was realized by crucible rotation. The metal Y was broken into small pieces (about 20 mm×20 mm×20 mm) with the total mass of 2.0 kg, and then they were put together into a copper crucible, as shown in Fig.2. Whereafter, the furnace door was closed and the vacuum system was operated. The equipment pressure was kept at $<5.0\times10^{-3}$ Pa for 15 min to remove air as much as possible. Then, the vacuum system ceased, and the flow control valve was turned on. The high purity Ar gas (> 99.9995%) was flowed into the furnace with the flowing rate of 5 L/min. At the same time, the automatic vacuum control system of the equipment was turned on to keep the equipment pressure at about 10^5 Pa. Under this condition, the melting power was controlled at 7.5 kW, and the high purity Ar was ionized into high temperature plasma. Then, the crucible was turned on for rotation at 2.4°/min (5 mm/min), and PZM treatment was conducted from 5 times to 10 times.

2 Results and Discussion

2.1 Calculation of impurity equilibrium distribution coefficient k_0

The principle of zone melting is the solubility difference of impurity elements in the solid and liquid phases of the base metal. With the solubility difference, the redistribution of

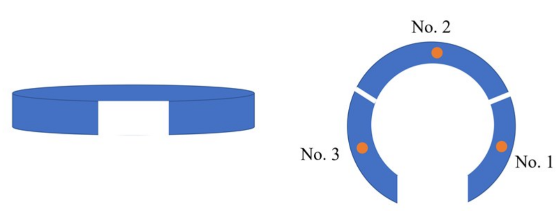

Fig.2 Schematic diagram of selected analysis points

impurity elements can be realized, thereby promoting the metal purification[22–23]. According to previous studies, the impurity equilibrium distribution coefficient k_0 is a key indicator to judge the moving direction of impurity elements, and its expression is as follows:

$$k_0 = \frac{C_s}{C_l} \tag{1}$$

where C_s and C_l are the concentrations of impurities in solid and liquid phases, respectively. When k_0<1, the corresponding impurities are enriched in the liquid phase; conversely, the impurities are enriched in the solid phase.

According to the principle of metal solidification[24], the equilibrium distribution coefficient of impurities in binary alloy system can be obtained by the liquid line and solid line of equilibrium state diagram. However, the solid phase line cannot be obtained accurately, which leads to the great difference in the state diagram of the same binary system, making it difficult to obtain the correct k_0 value. For this reason, the liquidus slope m_l and the crystallize latent heat ΔH_m are proposed to calculate the k_0 value, as follows:

$$k_0 = 1 + \frac{\Delta H_m}{RT_m^2} m_l \tag{2}$$

where ΔH_m is the latent heat of crystallization of the pure solvent component, J/mol; T_m is the melting point of the pure solvent component, K; m_l can be calculated by phase diagram of binary alloy; R is the gas constant. The equilibrium distribution coefficients of the common impurities Al[25], Si[26], Fe[27], Ni[28], Cu[29], and Mo[30] in metal Y can be calculated by Eq.(2), and the results are shown in Table 2. The related phase diagrams are shown in Fig.3.

According to Table 2, the k_0 values of the common impurities Al, Si, Fe, Ni, Cu, and Mo in metal Y are all less than 1. Therefore, in the PZM process, with the molten zone moving, the abovementioned impurities are enriched in the metal melt. As a result, the impurity content at the head side of ingot is lower than that at the tail side of ingot. The theoretical calculation results demonstrate that the abovementioned impurities can be effectively removed by PZM.

2.2 PZM process of metal Y

Fig.4 shows the Al and Si impurity distributions in metal Y after PZM process for 5 and 10 times along the moving direction of the molten zone, where x/L represents the location of sampling, x is the distance between the sampling point and the head side of the metal ingot, and L is the total length of the Y metal ingot. The sampling location is shown in Fig.2. After 5 and 10 times of PZM process, the samples at the head, middle, and tail positions of Y ingot were taken to analyze the variation of impurity content by ICP-OES. As shown in Fig.4a, the Al impurity content is increased gradually with the movement of the molten zone, and the impurity content at the same position is decreased with the increase in PZM process time. Similar result can be obtained for Si impurity in Fig.4b. Si also moves along the melting zoning direction and its redistribution is clearly related to the PZM process times. When the molten zone moves, Si content at the tail side is obviously lower than that at the head side. Therefore, the experiment results of the migration laws of Al and Si impurities are consistent with the theoretical results. Based on the equilibrium distribution coefficients of Al and Si impurities in Table 2, it is clear that the solubility of these two impurities in the metal Y solid phase is smaller than that in the liquid phase.

Table 2 Equilibrium distribution coefficient k_0 of common impurities in metal Y

Impurity	k_0	Phase diagram
Al	0.2173	Fig.3a
Si	0.2201	Fig.3b
Fe	0.5065	Fig.3c
Ni	0.1586	Fig.3d
Cu	0.1742	Fig.3e
Mo	0.8576	Fig.3f

Fig. 5 shows the Fe and Ni impurity distributions in metal Y after PZM process for 5 and 10 times along the moving direction of the molten zone. It is obvious that the migration laws of Fe and Ni impurities are consistent with those of Al and Si impurities, and they are also enriched at the tail side of ingot. The equilibrium distribution coefficients of Fe and Ni are also less than 1, which are 0.5665 and 0.1586, respectively. The experimental migration laws of Fe and Ni impurities agree with the theoretical results. These results also show the reliability of the theoretical results and suggest that Fe and Ni impurities can be removed by PZM process.

Fig. 6 shows the Cu and Mo impurity distributions in metal Y after PZM process for 5 and 10 times along the moving direction of the molten zone. The removal effect of the two impurities is improved with the increase in the PZM process time. The migration laws of Cu and Mo impurities are significantly affected by the equilibrium distribution coefficients k_0, which are 0.1742 and 0.8576, respectively. These k_0 values indicate that the impurities will migrate from the head side to the tail side with the molten zone moving, which agrees well with the experiment results. The Cu and Mo impurities are concentrated at the tail side of ingot.

2.3 Removal ratio

The content variation of impurity elements before and after PZM process and the influence of PZM process times on the removal ratio are further investigated. The removal ratio is expressed as follows:

$$R = \frac{C_0 - C_{min}}{C_0} \times 100\% \tag{3}$$

where R is the removal ratio, %; C_0 is the content of impurities in raw material; C_{min} is the lowest content of impurities after PZM process.

As shown in Fig.7a, PZM has a good removal effect on the

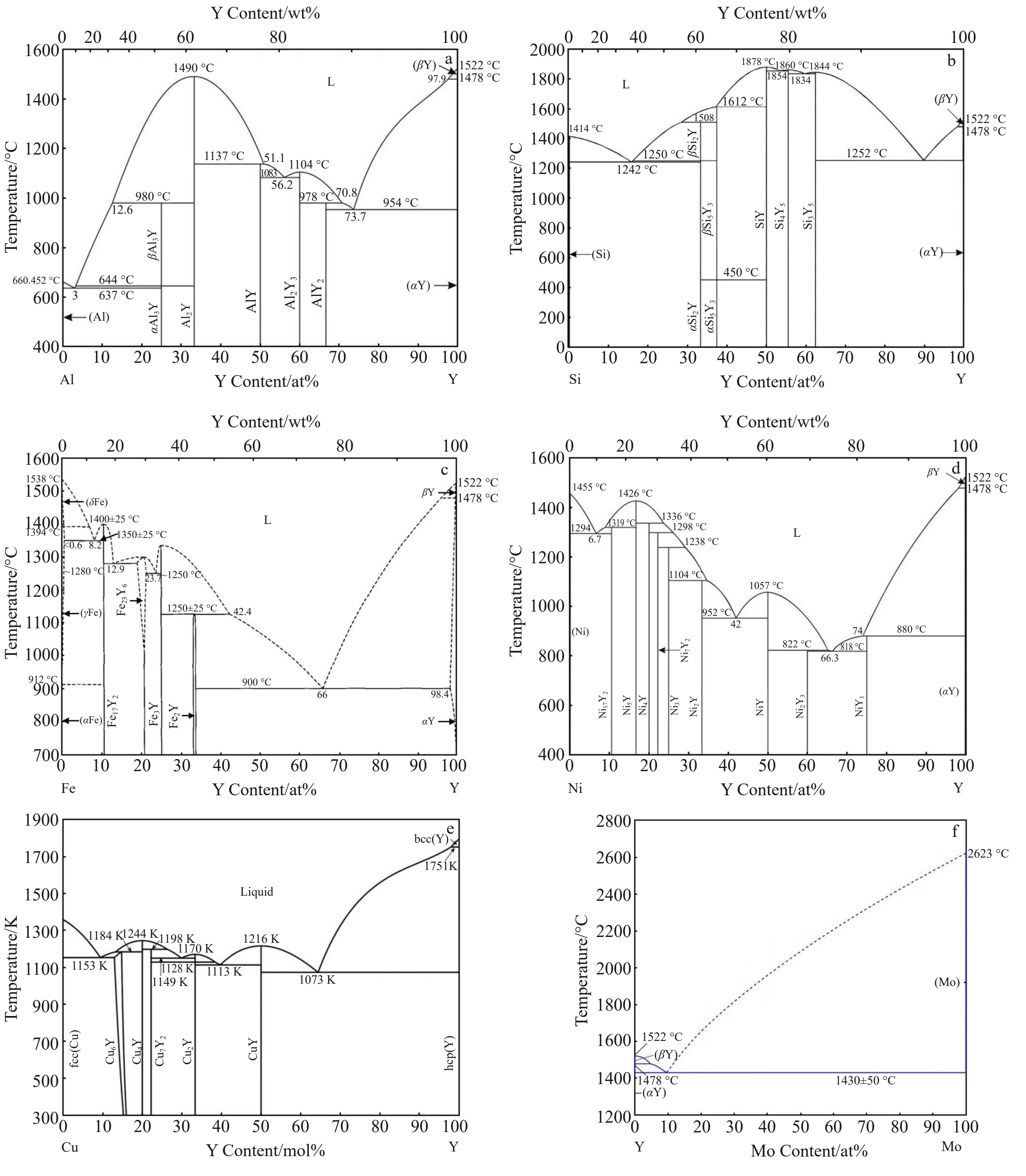

Fig.3 Phase diagrams of Y-Al (a), Y-Si (b), Y-Fe (c), Y-Ni (d), Y-Cu (e), and Y-Mo (f) binary alloys

refractory impurity elements Al, Si, Fe, Ni, Cu, and Mo, whose vapor pressure is close to or lower than that of metal Y. After PZM process for 10 passes, these impurities are all concentrated at the tail side of ingot, and their contents at the head side are the lowest. The contents of Al, Si, Fe, Ni, Cu, and Mo impurities are reduced from 0.014wt%, 0.0117wt%, 0.0103wt%, 0.0053wt%, 0.014wt%, and 0.0121wt% to 0.0076wt%, 0.0045wt%, 0.0068wt%, 0.0019wt%, 0.0067wt%, and 0.0065wt%, respectively. The removal ratios of the impurities at the head side after PZM process for 5 and 10 times are calculated by Eq.(3) and shown in Fig.7b. The results indicate that the removal ratio is increased with the increase in PZM process time. After PZM process for 10 times, the removal ratios of Al, Si, Fe, Ni, Cu, and Mo impurities are 45.71%, 61.54%, 33.98%, 64.15%, 52.14%, and 46.28%, respectively.

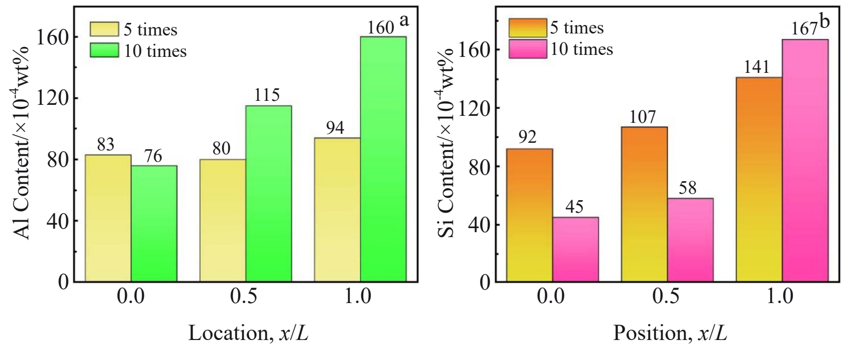

Fig.4 Al (a) and Si (b) impurity distributions in metal Y after PZM process for 5 times and 10 times

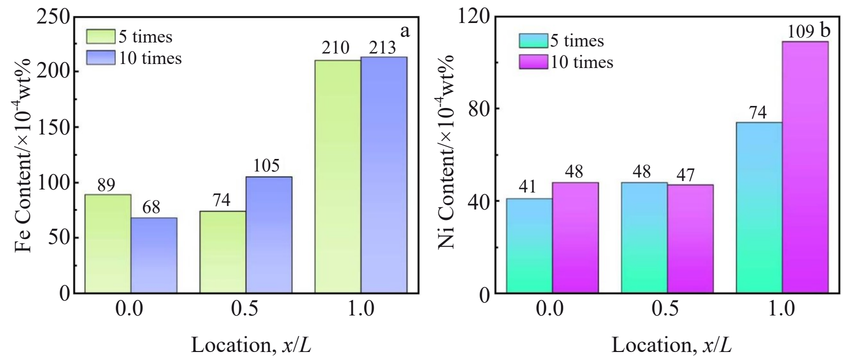

Fig.5 Fe (a) and Ni (b) impurity distributions in metal Y after PZM process for 5 times and 10 times

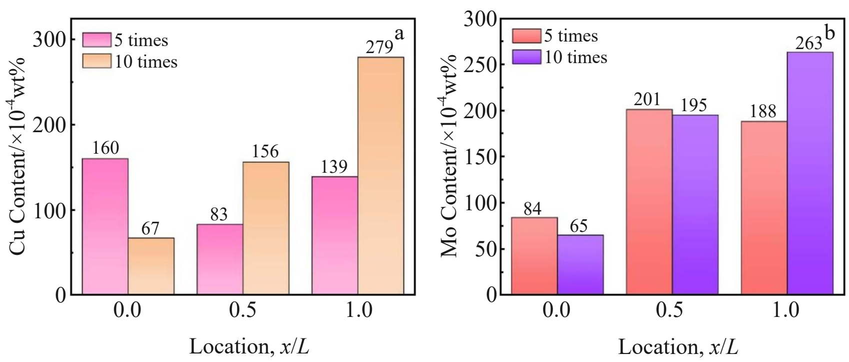

Fig.6 Cu (a) and Mo (b) impurity distributions in metal Y after PZM process for 5 times and 10 times

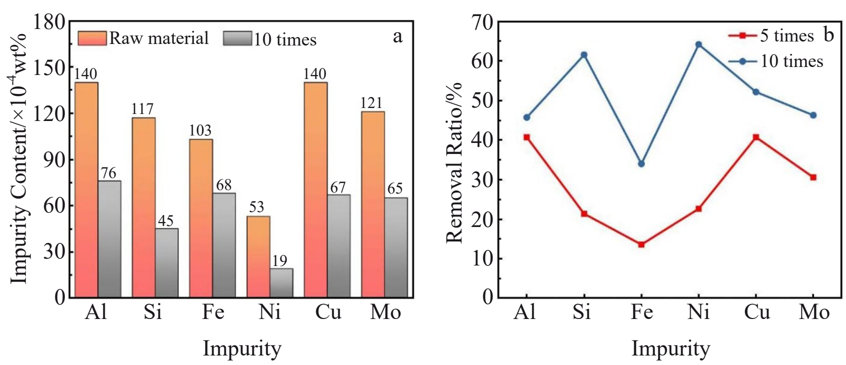

Fig.7 Impurity contents before and after PZM process for 10 times (a); removal ratio of impurities after PZM process for 5 times and 10 passes (b)

3 Conclusions

1) Based on the theoretical calculation, in the metal Y, the k_0 values of the common impurities Al, Si, Fe, Ni, Cu, and Mo are obtained as 0.2173, 0.2201, 0.5065, 0.1586, 0.1742, and 0.8576, respectively. Since their k_0 values are all less than 1,

when the molten zone moves, the abovementioned impurities will be enriched in the metal melt area after PZM process.

2) Experiment results verify the theoretical calculation results. Al, Si, Fe, Ni, Cu, and Mo impurities are all concentrated at the tail side of Y metal ingot, which is attributed to their high solubility in the liquid metal Y. The contents of these impurities are increased gradually with the movement of the molten zone. The removal ratio is increased with the increase in the PZM process time. After PZM process for 10 times, the removal ratios of Al, Si, Fe, Ni, Cu, and Mo impurities are 45.71%, 61.54%, 33.98%, 64.15%, 52.14%, and 46.28%, respectively.

References

1 Pang S M, Lu W L, Yang Z F *et al*. *Journal of Rare Earths*[J], 2021, 39(7): 875
2 Zhang Z Q, Wang Z Q, Miao R Y *et al*. *Vacuum*[J], 2014, 107: 77
3 Matsumoto Y, Nakatsuji S, Kuga K *et al*. *Science*[J], 2011, 331(6015): 316
4 Zhang T B, Chen Y G, Teng B H *et al*. *Materials Letters*[J], 2007, 61(2): 440
5 Macaluso R T, Nakatsuji S, Kuga K *et al*. *Chemistry of Materials*[J], 2007, 19(8): 1918
6 Fleck D C, Kleespies E K, Kesterke D G. *Purification of Yttrium by Electrorefining*[R]. Washington: Bureau of Mines, 1973
7 Hong J, Sun G Q. *Journal of Rare Earths*[J], 2006, 24(1): 362
8 Zhang Q, Li Q A, Chen J *et al*. *Advanced Materials Research*[J], 2013, 750–752: 603
9 Cao S T, Yang Y Q, Chen B *et al*. *Journal of Materials Science and Technology*[J], 2021, 86: 260
10 Liu L, Suwa Y, Sato S *et al*. *Japanese Journal of Applied Physics*[J], 2017, 56(4S): 04CJ02
11 Afanaseva I A, Bobkov V V, Gritsyna V V *et al*. *Vacuum*[J], 2016, 129: 148
12 Luo Y L, Zhang D F, Hua J R *et al*. *Rare Metal Materials and Engineering*[J], 2022, 52(1): 54
13 Zhang Y J, Du J H, Ji Q X *et al*. *Rare Metal Materials and Engineering*[J], 2022, 51(10): 3588
14 Daane A H, Spedding F H. *Journal of the Electrochemical Society*[J], 1955, 100(10): 442
15 Carlson O N, Haefling J A, Schmidt F A *et al*. *Journal of the Electrochemical Society*[J], 1960, 107(6): 540
16 Yang S H, Yang F L, Liao C F *et al*. *Journal of Rare Earths*[J], 2010, 28(1): 385
17 Volkov V T, Ionov A M, Nikiforova T V. *Vacuum*[J], 1999, 53(1–2): 105
18 Volkov V T, Nikiforova T V, Ionov A M *et al*. *Journal of the Less Common Metals*[J], 1981, 79(2): 199
19 Habermann C E, Daane A H. *Journal of the Less Common Metals*[J], 1962, 5(2): 134
20 Okabe T H, Deura T N, Oishi T *et al*. *Journal of Alloys and Compounds*[J], 1996, 237(1–2): 150
21 Yaws C L, Satyro M A. *The Yaws Handbook of Vapor Pressure*[M]. Cambridge: Gulf Professional Publishing, 2015: 315
22 Wan H L, Xu B Q, Yang B *et al*. *Vacuum*[J], 2019, 171: 108839
23 Lv G Q, Chen D T, Yang X *et al*. *Vacuum*[J], 2015, 116: 96
24 Hu Hanqi. *Principle of Metal Solidification*[M]. Beijing: China Machine Press, 2000 (in Chinese)
25 Liu S H, Yong D, Xu H H *et al*. *Journal of Alloys and Compounds*[J], 2006, 414(1–2): 60
26 Shukla A, Kang Y B, Pelton A D. *International Journal of Materials Research*[J], 2009, 100(2): 208
27 Fan L, Shen C, Hu K *et al*. *Journal of Phase Equilibria and Diffusion*[J], 2021, 42(3): 348
28 Mezbahul-Islam M, Medraj M. *Calphad*[J], 2009, 33(3): 478
29 Guo C P, Liu K Q, Li C R *et al*. *Calphad*[J], 2020, 70: 101775
30 Massalski T B. *Binary Alloy Phase Diagrams*[M]. Ohio: ASM International, 1990

等离子区域熔炼提纯金属Y过程中的杂质迁移规律

徐明磊[1,2]，卢文礼[2,3,4]，张小伟[1,2,3]，陈德宏[1,2]，李金颖[2]，余 创[1,2]，杨文晟[2,3]，王志强[1,2]

(1. 有研稀土高技术有限公司，河北 廊坊 065201)

(2. 有研稀土新材料股份有限公司，北京 100088)

(3. 稀土国家工程研究中心，北京 100088)

(4. 北京科技大学 冶金与生态工程学院，北京 100083)

摘 要：利用等离子体区域熔炼提纯金属钇，获得了区熔提纯过程中Al、Si、Fe、Ni、Cu和Mo等杂质的迁移规律。计算结果表明，金属钇中Al、Si、Fe、Ni、Cu和Mo等常见杂质的平衡分配系数分别是0.2173、0.2201、0.5065、0.1586、0.1742和0.8576。由于上述杂质平衡分配系数小于1，杂质在液相中的溶解度大于固相溶解度，所以从理论上可判断出Al、Si、Fe、Ni、Cu和Mo等杂质将随着熔区移动富集在金属钇锭的尾端，也就是最后凝固区。实验结果证明了该理论预判的准确性。此外，探究了区熔次数与杂质迁移的内在联系，结果表明：随着区熔次数由5次增加至10次，杂质在金属钇锭尾端富集程度增加，即去除率升高。10次区熔后，Al、Si、Fe、Ni、Cu和Mo等杂质的去除率分别为45.71%、61.54%、33.98%、64.15%、52.14%和46.28%。由于上述杂质饱和蒸气压与金属钇接近，所以很难通过常规方法予以去除。等离子体区域熔炼提纯金属钇的研究为制备高纯钇提供了一种新方向。

关键词：迁移规律；等离子体区域熔炼；分配系数；钇；去除效率

作者简介：徐明磊，男，1994年生，有研稀土高技术有限公司，河北 廊坊 065201，电话：010-61590666-8212，E-mail：xuminglei@grirem.com